INFLUENCE OF TURBULENCE ON THE EFFICIENCY AND RELIABILITY OF COMBUSTION CHAMBER OF THE GAS TURBINE

by

Samal B. SADYKOVA[a]***, Abay M. DOSTIYAROV***[a]***,***
Mikhail G. ZHUMAGULOV[b*]***, and Nurlan R. KARTJANOV***[b]

[a] Gumarbek Daukeev Almaty University of Power Engineering and Telecommunications, Almaty, Kazakhstan
[b] L. N. Gumilyov Eurasian National University, Nur-Sultan, Kazakhstan

Original scientific paper
https://doi.org/10.2298/TSCI200831064S

The article presents the research results related to the influence of turbulence on the efficiency of the combustion chamber of gas turbine. An artificial increase in the intensity of turbulence is considered as a way to improve the formation of a fuel-air mixture. Turbulent flow is formed due to the installation of guide swirlers at the entrance to the device for creating a fuel-air mixture – a micro module. The angle of rotation of the swirler blades is selected. Theoretical research, mathematical software modelling, as well as an aerodynamic experiment have been carried out. As a result, design solutions are provided that significantly increase the efficiency and reliability of the gas turbine combustion chamber. In the course of the study, guide vanes were selected, and their design was established. The recommended swing angle of the swirler guide vanes is 40°. The recommended depth of the fuel injector inside the chamber is 1.0 gauge.

Key words*: combustion chamber, gas turbine, turbulence, turbulence intensity, swirl flow, thermal anemometer, airstream atomizer*

Introduction

Objective

Due to the intense population growth, the demand for electricity has led to a new wave of research in the energy sector. To generate and transport energy, a large amount of fuel must be burned [1]. Gas turbines are one of the most advanced heat engines today. The combustion chamber is the heart of a gas turbine engine, therefore, its design is critical for the stability of the engine as a whole under various loads. As efficiency and emission standards become more stringent, gas turbine manufacturers are looking to improve efficiency and reduce emissions using a variety of methods. For example, combustion of a lean air-fuel mixture is one of the latest concepts [2-8]. In the mid 1970's, General Electric began developing the Dry low NO_x concept and introduced it into its combustion chamber design [9, 10]. These combustion chambers were aimed at reducing the flame temperature by burning fuel in the poorest depleted conditions in the main zone, which leads to a decrease in thermal NO_x emissions.

This method of organizing the combustion process in the combustion chambers simultaneously provides a high completeness of fuel combustion, but at the same time greatly reduc-

* Corresponding author, e-mail: Zhmg_9@mail.ru

es its reliability and the range of loads of stable operation [11-13]. A decrease in the reliability and stability of the combustion chamber is associated with the following:

- flame breakthrough, due to which thermal destruction and burnout of the fuel of combustion devices occurs,
- poor flame-out, which causes pressure pulsations and mechanical stress on the parts of the combustion chamber and turbine,
- the formation of a fuel-rich hearth in the flame, which is the main reason for the existence of local hot zones,
- in traditional burners, due to the uneven temperature field, the guide vanes of the first stage of the gas turbine fail, and
- when the load is reduced, there is a danger of flame breakdown and flame breakthrough.

To eliminate these disadvantages, the authors propose multi-nozzle combustion technology [14] as the first provision, which will provide high efficiency, environmental friendliness and operational reliability. The technology consists in dividing the entire lean mixture flow and feeding it through a series of micromodular channels instead of one large inlet pipe. The total cross-sectional area of all micromodules is selected equal to the cross-sectional area of the former monochannel, which allows maintaining the same flow rate. The technology makes it possible to evenly distribute fuel throughout the entire combustion volume and to better mix fuel and combustion air. In a traditional directional injection chamber, fuel is delivered in one stream. A high concentration of fuel is created in local areas. As a consequence, it takes longer to mix with the air, resulting in higher emission levels. Thus, the division and injection of the fuel volume into several smaller micromodules instead of one large one will provide the required flow rate, but with a better distribution in the space of the combustion chamber. In support of this, a number of studies [15-21] describe the positive impact of multi-injection technology on performance using diesel engines as an example.

Subject of research

The second and main point of the current research is the improvement of mixing in each separately taken micromodule. The obvious solution is a swirling stream. Swirling flame is the main type used in gas turbine engines. It provides a compact heat release, stabilization and ignition in a wide range of the initial mixture [22, 23]. The vortex flame provides a high level of turbulence that promotes good mixing, allowing the use of smaller combustion chambers. Thus, the efficiency of mixing and fuel-air mixture formation is a function of the turbulence of the flow. The authors of this work set themselves the task of increasing turbulence while maintaining the stability of the combustion chamber. For this purpose, the design of a micromodular airstream nozzle (MMAN) [24] is proposed, fig. 1. It contains a cylindrical body with an inner diameter D = 46 mm and a length of 150 mm, in which a swirler (register) with eight blades with equal angles of rotation of the blades β_1 and a fuel supply pipe along the horizontal axis are installed. At the exit from the cylinder, two registers are sequentially installed with β = 30° and 20° angle, respectively.

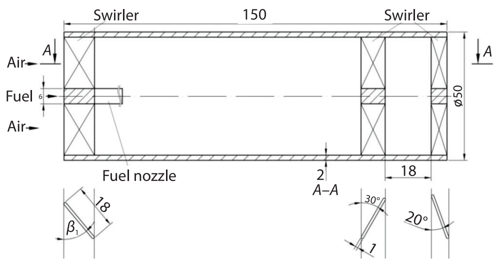

Figure 1. The MMAN

The special design of the burner operates as follows. Part of the air enters the microchamber in a swirling flow through the inlet swirler. The amount of air is selected less than that required for ignition. Fuel is supplied through an axial channel buried in the micromodule (fuel nozzle). The intracylindrical space forms a zone for preliminary preparation of the *poor* fuel – air mixture with excess fuel. The main combustion zone is localized at the exit from the MMAN. The first one downstream of the outlet swirlers ensures the homogenization of the mixture and the intensification of mass transfer, and also, together with the second register, prevents the propagation of the flame inside the microchamber. At the exit from the MMAN, the homogeneous mixture enters the combustion chamber, where it intensively mixes with the main air-flow and begins to burn. As a result of re-circulation of gaseous streams, turbulence and significant shear between re-circulation zones, mixing is improved and premixed states are quickly achieved. If the fuel nozzle is mounted with a projection relative to the chamber surface, this distance helps to achieve a mixed state before the reactants are transferred to the base of the flame [25].

As a result, the purpose of this study is to optimize the design of a micromodular nozzle with an increase in turbulence and the intensity of the formation of a fuel-air mixture. For this, the following problems were solved by mathematical modelling and cold experiment:
– Defining the effective angle of rotation of the inlet swirler blades β_1.
– Determination of the degree of penetration of the fuel supply nozzle into the micromodule.

Further, a mathematical model and experimental studies of the intensity of turbulence of the isothermal flow inside the micromodule at different angles of the blades are carried out.

Numerical and experimental methodology

The concept of turbulence

We should remind that turbulence is characterized by a chaotic random motion of gas particles, as well as a high level of vortex oscillations and dissipation of its kinetic energy. This property does not apply to the fluid itself, but to its flow. The main characteristics of turbulence are independent of the molecular properties of the liquid. Turbulence is a continuous phenomenon described by the equations of fluid dynamics, the Navier-Stokes equation, which can be dimensionless, leaving the Reynolds number as the only independent parameter [26]. The equation has no general solution, and therefore, experimental or numerical research methods are used in engineering practice [27].

Governing equations

The main formulas are in the complete equations of conservation of mass, momentum and energy in Cartesian co-ordinates:

$$\frac{\partial \rho}{\partial t}+\frac{\partial \rho u_i}{\partial x_i}=0 \tag{1}$$

$$\frac{\partial \rho u_i}{\partial t}+\frac{\partial(\rho u_i u_j)}{\partial x_j}=-\frac{\partial p}{\partial x_i}+\frac{\partial \tau_{ij}}{\partial x_j} \tag{2}$$

$$\frac{\partial \rho E}{\partial t}+\frac{\partial\left[(\rho E+p)u_i\right]}{\partial x_i}=-\frac{\partial q_i}{\partial x_i}+\frac{\partial\left(u_i\tau_{ij}\right)}{\partial x_j} \tag{3}$$

where ρ [kgm^{-3}] is the density, u [ms^{-1}] – the velocity, t [s] – the time, x [m] – the spatial co-ordinate, p [Pa] – the pressure, τ_{ij} [kgm$^{-1}s^{-2}$)] – the viscous stress tensor, and E – the specific total energy is defined:

$$E = e + \frac{u_i u_i}{2} \tag{4}$$

$$e = h - \frac{p}{\rho} \tag{5}$$

$$h = h_{\mathrm{ref}} + \int_{T_{\mathrm{ref}}}^{T} C_p \mathrm{d}T \tag{6}$$

where e [Jkg^{-1}] is the specific internal energy, h [Jkg^{-1}] – the enthalpy, h_{ref} [Jkg^{-1}] – the reference enthalpy, C_p [Jkg^{-1}K^{-1}] – the isobaric heat capacity, T [K] – the temperature, and T_{ref} [K] – the reference temperature.

We apply the equation of state for an ideal gas:

$$p = \frac{\mathrm{R_u} \rho T}{m} \tag{7}$$

where universal gas constant is $\mathrm{R_u}$ = 8314.36 J/(kmol·K) and m is the molar mass. The Newtonian fluid and Stokes assumptions are implemented for the viscous stress tensor, τ_{ij}:

$$\tau_{ij} = -\frac{2}{3}\mu \frac{\partial u_{\mathrm{k}}}{\partial x_{\mathrm{k}}} \sigma_{ij} + \mu \left(\frac{\partial u_j}{\partial x_i} + \frac{\partial u_i}{\partial x_j} \right) \tag{8}$$

where μ [kgm^{-1}c^{-1}] is the viscosity, k – the Kolmogorov scale, and σ – the Kronecker delta function.

Choosing a turbulence model

The ANSYS FLUENT provides a wide range of built-in models for specific classes of problems. The choice of a turbulence model depends on the required level of accuracy, available computing resources and the required processing time. The most suitable turbulence model for the study under consideration is the shear-stress transport (SST) k-ω-model.

The k-ω model with SST was developed by Menter [28]. It is so named because the definition of turbulent viscosity has been transformed to take into account the transfer of the main shear of turbulent stress. The shift has a feature that gives the SST k-ω -model a performance advantage over both the standard k-ω model and the standard k-ε model. Other options include adding a cross-diffusion variable to the equation ω and a mixing function confirm the similarity of the behavior of the model equations in both the near-wall and other zones [29].

The SST k-ω has a shape similar to the standard k-ω. The kinetic energy of turbulence k and the specific dissipation rate ω are obtained from the transport equations:

$$\frac{\partial \rho k}{\partial t} + \frac{\partial \rho k u_i}{\partial x_i} = \frac{\partial}{\partial x_j} \left(\mathit{\Gamma}_k \frac{\partial k}{\partial x_j} \right) + \tilde{G}_k - Y_k + S_k \tag{9}$$

$$\frac{\partial \rho \omega}{\partial t} + \frac{\partial \rho \omega u_i}{\partial x_i} = \frac{\partial}{\partial x_j} \left(\mathit{\Gamma}_\omega \frac{\partial \omega}{\partial x_j} \right) + G_\omega - Y_\omega + D_\omega + S_\omega \tag{10}$$

The calculations of all the listed variables are fully described in [29].

The basic equations are solved numerically using the finite volume method. This method allows arbitrary geometry to be handled and avoids the metric issues commonly associated with finite difference methods. To initiate the finite volume method, we first integrate the conservation equations over a small control volume, V, bounded by surface, S. Then the volume integral for the flux vector is transformed into a surface integral using the Gaussian divergence theorem.

Computer modelling approach

During the simulation, the following parameters were selected for the main analysis: flow velocity, u, and turbulence intensity, ε.

In the course of the simulation, the angle of rotation of the blades β_1 of the air swirler at the inlet changed in accordance with the values of 20°, 30°, 40°, and 60°.

Experimental approach

Thermal anemometry was chosen as a method for measuring the intensity of turbulence. A constant temperature anemometry system is used to study the characteristics of the cold flow leaving the burner. The thermo anemometer measures the velocity of the flow field by detecting changes in heat transfer from the sensor to the ambient air, which is limited. An electrically heated wire with a diameter of four to six microns is exposed to an air channel in the burner. The decrease in sensor temperature due to air-flow is balanced by a current to maintain a constant temperature, and this current is calibrated to measure the flow rate.

Similarly with the mathematical model, two indicators were studied in the experiment: the intensity of turbulence and the velocity characteristic of the air-flow inside the MMAN at different angles of installation of the blades of the inlet swirler β_1.

The experiment was carried out on a stand, the diagram of which is shown in fig. 2. The stand consists of a fan for air supply, a wind tunnel, at the outlet of which an MMAN with a calibration tube (Witoszinski nozzle) and a constant temperature thermal anemometer are installed. The sensing element of the thermal anemometer is a tungsten filament sensor.

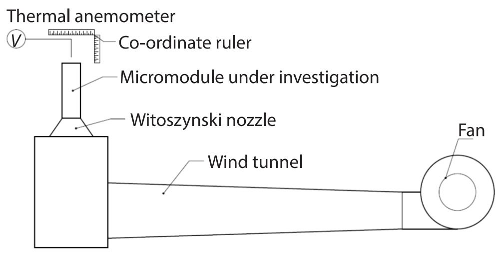

Figure 2. Experimental set-up

The first stage of the experiment is the calibration of the thermal anemometer at different flow rates at the outlet from the Witoszynski nozzle in front of the MMAN. For this, a Pitot tube was installed in the center of the nozzle, according to the value of which the dependence on the speed $E = f(u)$ was determined at different fan performance.

Then, using a thermal anemometer, the readings of the MMAN were measured at various points and the turbulence intensity was calculated using the eq. (11). Calibers 0, 0.5, 1, and 1.5 were chosen as the measurement points with a step of 5 mm along the cross-section of the MMAN. The inner diameter of the micromodule is taken as one gauge, and the steps moved horizontally relative to the longitudinal axis of the micromodule.

According to the readings of the thermal anemometer at the points under study, the turbulence intensity was calculated [27]:

$$\varepsilon = \frac{4\overline{E}(\overline{e} - e_0)}{\overline{E}^2 - \overline{E}_0^2} \times 100\% \tag{11}$$

The average flow rate $\bar{u}$ of the selected points inside the micromodule was determined on the basis of the dependence $E = f(u)$:

$$\overline{u} = \left(\frac{\overline{E}^2 - A}{B} \right)^2 \tag{12}$$

where A, B are the coefficients of the calibration dependence, which are determined from the graph $E = f(u)$ [27].

Results

Modelling results

Figure 3 shows the distribution of the flow rate of the gas-air mixture through the proposed micromodule.

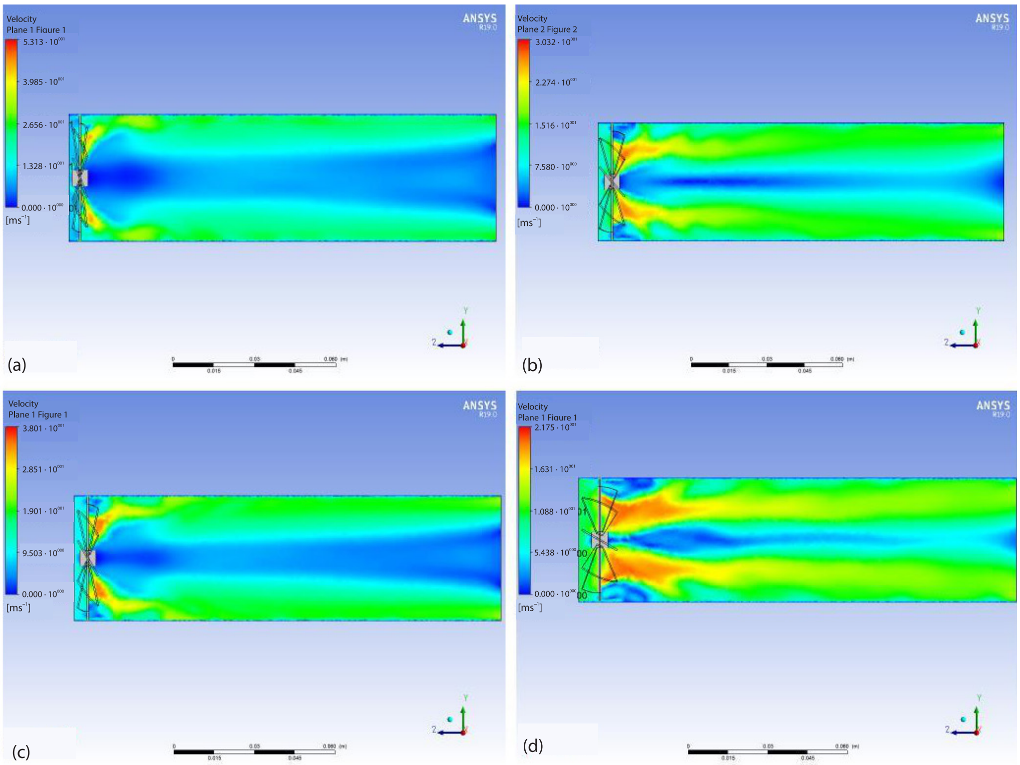

Figure 3. Velocity distribution in the micromodule; (a) β = 20°, (b) β = 40°, (c) β = 30°, and (d) β = 60°

Let us consider the general trends and features of each individual case.

The minimum speed is observed in the axial zone. In some areas, the value approaches zero. This is easily explained by the fact that the main air mass, in addition the vortex motion, also has a centrifugal one. The deceleration of the flow on the axis at the entrance is the result of a physical obstacle in the form of a fuel nozzle. At small angles β_1 (20-30°), the main flow of inlet air is sharply redirected to the walls of the micromodule, pressing against them, and then moves in the near-wall region, braking against the passive central flow. The maximum value of the velocities is distributed along the periphery of the open section. The thickness of the near-wall high speed zone increases with an increase in the angle β_1 against the background of a reduction in the axial space of low speed. The peak velocity of 20-50 m/s takes place directly near the swirler (confuser effect). The main conclusion based on fig. 3: the larger the angle β_1, the more completely the chamber is filled with a high velocity flow. The most preferable option is β_1 = 40°, since this case demonstrates the most uniform distribution of the speed over the chamber at a level of 1.6 m/s, in contrast to the variant with $\beta_1 = 60°$, where peaks and unevenness of speeds can lead to instability of the micromodule operation in the whole.

Turbulence parameters are shown in fig. 4.

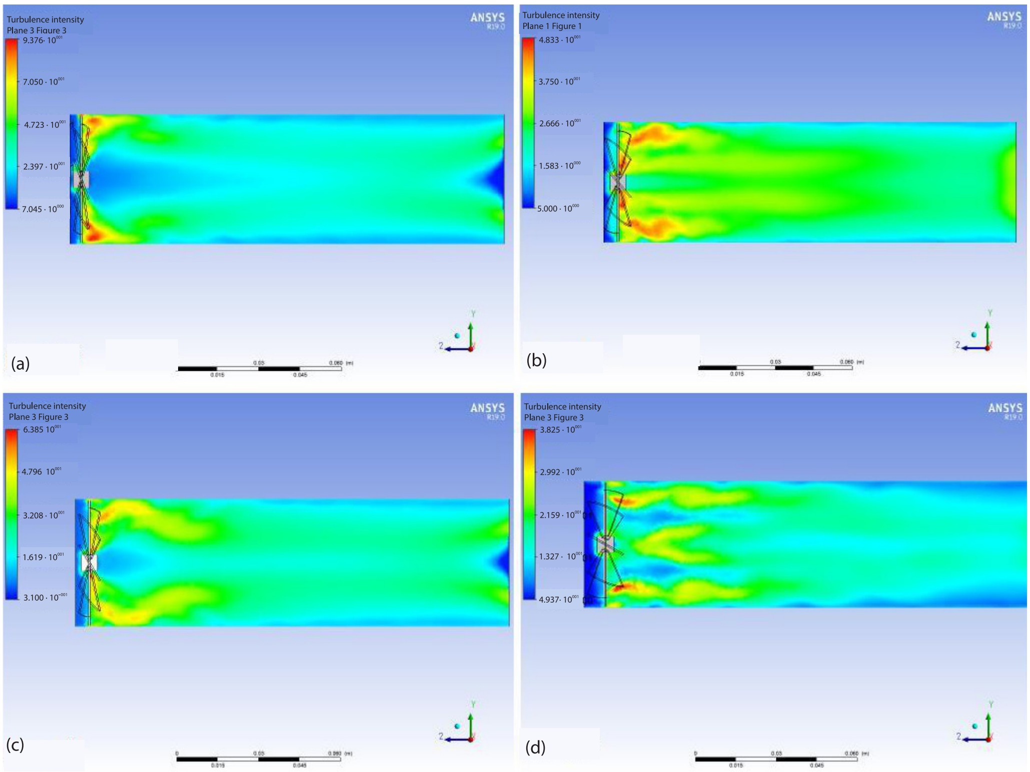

Figure 4. Turbulence intensity; (a) β = 20°, (b) β = 40°, (c) β = 30°, and (d) β = 60°

As expected, turbulence is distributed over the micromodule similarly to the velocity distribution, since it is a derivative of it. In the axial zone, the values tend to 1, which indicates low turbulence or none at all. Closer to the walls, the intensity increases. The thin boundary-layer near the walls also has a low intensity as a result of the natural deceleration of the flow against the wall. The input register forms a zone of maximum intensity after itself. With an increase in the angle β_1, the zone of intense turbulence stretches into the depth of the chamber. In the case with an angle $\beta_1 = 60°$, the main flow rupture with the formation of two centers of turbulence, the values of which do not exceed the average intensity level for the case with $\beta_1 = 40°$.

Recall that the authors of the article seek to achieve a high intensity of turbulence, distributed as much as possible over the entire volume of the chamber. Based on this problem, $\beta_1 = 40°$ *is considered the optimal angle. This angle of rotation of the inlet swirler blades provides the most uniform field of turbulence intensity and flow velocity over the chamber volume*. An additional factor in favor of choosing the angle $\beta_1 = 40°$ is a smooth increase in turbulence towards the outlet section, which will have a positive effect on the combustion conditions when the lean mixture leaves the micromodule.

Figure 3(b) shows that the edge of the transition of peak values to uniform velocities falls on the cross-section of one caliber deep into the chamber (50 mm from the edge of the micromodule). Figure 4(b) also confirms this. As a result, *the authors of the article recommend to mount a fuel nozzle with a projection of 1.0 caliber inward relative to the front surface of the chamber. The fuel supply is recommended not axially, but radial for better capture of fuel by air masses. Such a device will contribute to improved formation of a fuel-air mixture.*

For more accurate and scientifically substantiated conclusions, in confirmation or denial of the obtained results, a *cold* experiment was carried out at the extreme stage of the study.

Experimental results

The results of measurements of the average flow rate and turbulence intensity at selected points using eqs. (11) and (12) are shown in figs. 5 and 6.

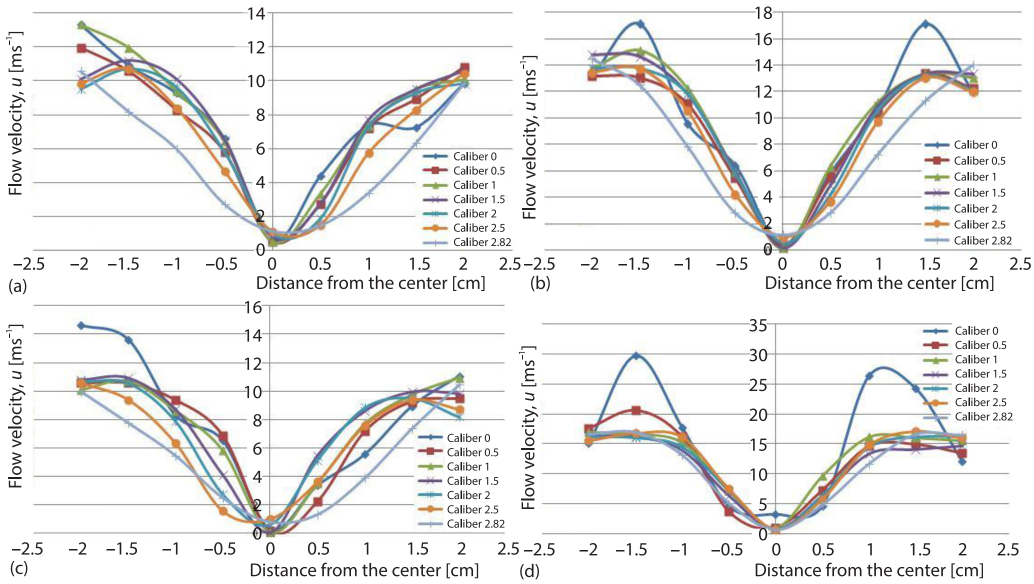

Figure 5. Flow rate inside the micromodule

The tendencies in the distribution of velocities over the cross-section of the micromodule with a sufficient degree of reliability repeat the data obtained during the simulation. On the axis in most calibers, the flow tends to slow down. The speed increases towards the periphery. Natural deceleration of the flow occurs in the boundary-layer near the wall. With an increase in angle β_1 on the axes of micromodules, the zone with a low flow rate decreases and the thickness of the layer with a high one increases.

As the processing of experimental data shows, the minimum value of the turbulence intensity, ε, falls on the axis. The maximum values are noted at a distance of 0.5 cm from the center in all angles of the swirlers. On the cross-section of the micromodule, the main intensity zone is concentrated on the outer layers (0.5-2.5 cm from the center). This is due to the fact that with a swirling flow, due to centrifugal forces, the flow is concentrated at the periphery and a zone with a low average velocity appears in the center of the micromodule, and, therefore, turbulent pulsations in this zone are reduced. According to eq. (3), the intensity is formed by pulsations of the average velocity, and therefore, the incoming flows from the center to the wall

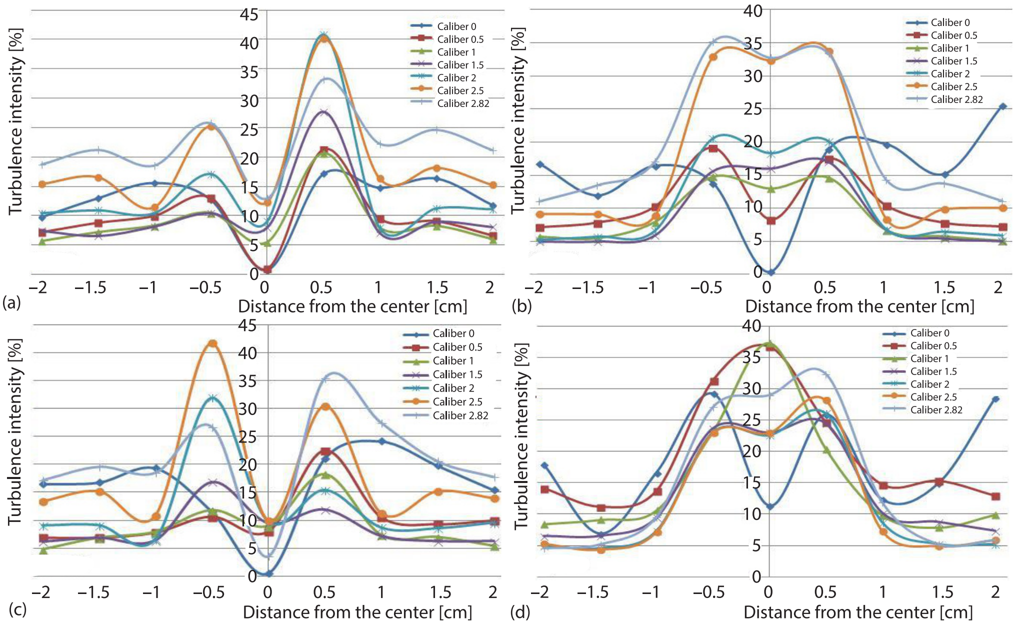

Figure 6. Intensity of turbulence inside the micromodule

create high pulsations. The outermost layer near the walls shows a decrease in intensity, which is a consequence of the deceleration of the flow in the near-wall region.

The average ε along the longitudinal section increases towards the output of the micromodule, which is demonstrated by the measurement points for different calibers. Intensity equalization in the axial zone starts at 1.0 gauge. As aforementioned, the fuel supply is supposed to be carried out into this section at a distance of approximately one caliber (46-50 mm). Therefore, turbulence in this zone will play a decisive role in the formation of the fuel-air mixture.

Let us analyze the influence of the swirler blades setting angle on the turbulence intensity. As can be seen from the graph, at $\beta_1 = 20°$ ε in the center of the micromodule at calibers 0.5, 1 is 25-28% and decreases towards the micromodular wall to 5%. The maximum flow velocity is observed at the periphery and decreases towards the center of the micromodule to 0.2-0.4 m/s, which means that the air-flow is concentrated at the periphery.

At $\beta_1 = 30°$, the turbulence intensity range at the same points is 30-32%. At the periphery in the range from 4.79-10%. Here, at $\beta = 30°$, the flow rate is also concentrated on the inner periphery of the micromodule, but the layer thickness increases at a high rate.

With an increase in the blade angle β in the central part of the micromodule, ε increases; at $\beta_1 = 40°$ and $\beta_1 = 60$ °, the average ε at the maximum is 34% and 37%, respectively. The flow rate curves show that with an increase in the angle on the axes of the micromodules, the zone with a low flow rate decreases and the layer thickness increases at a high rate. Also, at $\beta_1 \geq 40°$, relatively uniform volumetric turbulence is observed than at $\beta_1 \leq 40°$. This is due to the fact that at low angles of installation of the swirlers there is a strong radial swirl of the flow and a decrease in the axial component of the flow velocity.

Discussion

The obtained results of mathematical modelling and cold experiment obviously confirm each other. There is a single tendency for the variable to change depending on the co-ordinate.

Checking the mathematical model for reliability by conducting an experiment on the entire data set is very cumbersome and it is not possible to be fully present in the article. Obviously, the cross-section of a micromodule with a caliber of 1.0 at a swirler blade rotation angle β_1 of 40° is of the greatest interest for research. This section is most favorable for fuel supply. Therefore, we will consider the issues of convergence of the study using the example of this section, fig. 7.

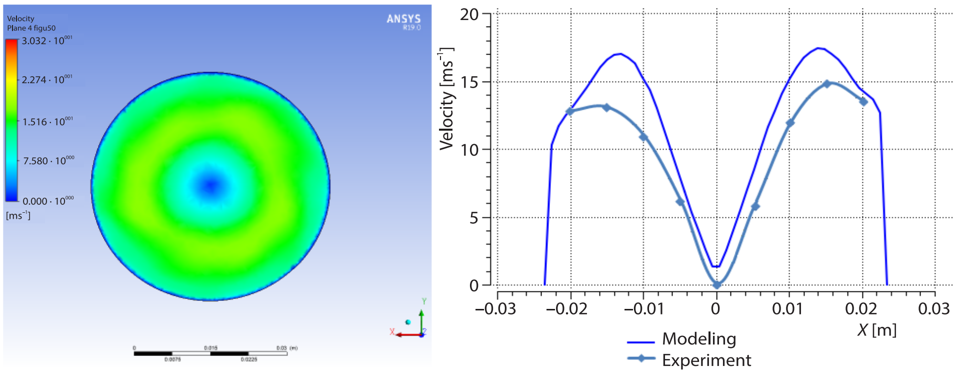

Figure 7. Section of a micromodule with a caliber of 1.0 at β_1 = 40°

The relative measurement error is based on comparing the data of computer modelling and experiment. The relative measurement error δ [%] was determined as:

$$\delta = \frac{\Delta u}{u_{\mathrm{exp}}} \times 100\% = \frac{u_{\mathrm{mod}} - u_{\mathrm{exp}}}{u_{\mathrm{exp}}} \times 100\% \tag{13}$$

where u_{mod} [ms^{-1}] is the velosyty from the computer modelling data and u_{exp} [ms^{-1}] – the velosyty from the experiment.

The velocity graph shows that the discrepancy in values increases closer to the periphery and reaches a maximum value of 22% at around 1.5 cm from the center. The average error over the entire section is 12.4%. The experimental data are almost uniformly underestimated over the entire area relative to the curve of the mathematical model. A similar effect occurs in measurements when there is a systematic error. If we correct for systematic error, then the maximum relative error decreases to 14.5% with its average value of 6.9%. Figure 8 shows the relative error before fig. 8(a) and after fig. 8(b) the correction. The absolute error of the speed on the micromodule axis (mark 0) is taken as the correction value and is 1.32 m/s. In other words, the experimental curve in fig. 7 will rise 1.32 points higher.

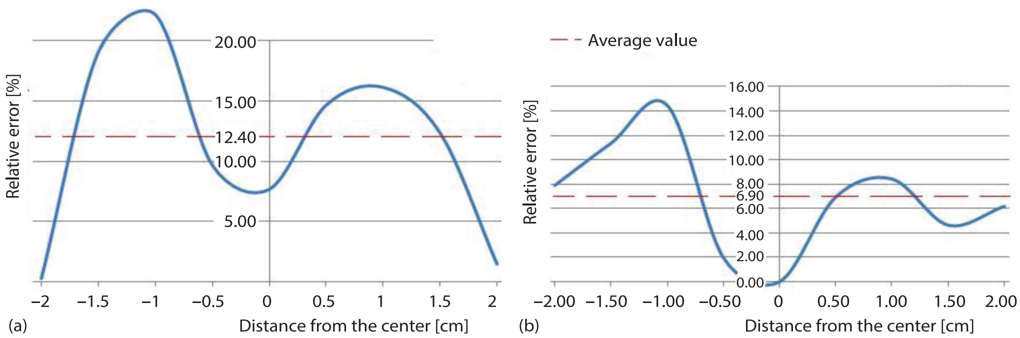

Figure 8. Relative measurement error for a section of a micromodule with a caliber of 1.0 at β_1 = 40°; (a) before the introduction of the correction and (b) after adjustment

Conclusion

In accordance with the data presented, in order to achieve a high turbulence intensity, distributed as much as possible over the entire chamber volume, the optimal angle $\beta_1 = 40°$ is recommended. This angle of rotation of the inlet swirler blades provides the most uniform field of turbulence intensity and flow velocity over the chamber volume. An additional factor in favor of choosing the angle $\beta_1 = 40°$ is a smooth increase in turbulence towards the outlet section, which will have a positive effect on the combustion conditions when the lean mixture leaves the micromodule.

The edge of the transition of peak values to uniform velocities falls on the cross-section of the caliber 1.0 deep into the chamber (46-50 mm from the edge of the micromodule). The authors of the article recommend mounting a fuel injector with a 1.0 caliber protrusion inward relative to the front surface of the chamber. The fuel supply is recommended not axially, but radial for better capture of fuel by air masses. Such a device will contribute to improved formation of a fuel-air mixture.

This is a qualitative assessment of the proposed device. In order to quantify the work of the micromodule, it is necessary to simulate and conduct a hot experiment with mandatory measurement of NO_x emissions. Reducing the level of harmful emissions is the main indicator of the quantitative assessment of the operation of the device. This study is planned for the next stage.

Nomenclature

A, B – coefficients of the calibration, model constants, [–]
C_p – isobaric heat capacity, [Jkg^{-1}K^{-1}]
D_ω – an indicator of interdiffusion, [m^{2}s^{-1}]
E – specific total energy, [Jkg^{-1}]
$\bar{E}_0$ – bridge stress with no flow in the pipe, [B]
$\bar{E}$ – constant component of bridge stress with flow in a pipe, [B]
e – specific internal energy, [Jkg^{-1}]
e_0 – system error, [B]
$\bar{e}$ – variable (ripple) component of the bridge stress at flow in the pipe, [B]
G_ω – generation ω, [–]
$\bar{G}_k$ – generation of kinetic energy of turbulence due to average velocity gradients, [–]
h – enthalpy, [Jkg^{-1}]
h_{ref} – reference enthalpy, [Jkg^{-1}]
k – kinetic energy of turbulence [J]
p – pressure, [Pa]
R_u – universal gas constant [Jkmol^{-1}K^{-1}]
S_k, S_ω – user-defined source variables, [–]
T – temperature, [K]
T_{ref} – reference temperature, [K]
t – time, [c]
u – velocity, [ms^{-1}]
x – spatial co-ordinate, [m]
Y_k, Y_ω – dispersion of k and ω due to turbulence, [–]

Greek symbols

Γ_k, Γ_ω – effective diffusion coefficient k and ω, respectively, [m^{2}s^{-1}]
μ – viscosity, [kgm^{-1}s^{-1}]
ρ – density, [kgm^{-3}]
σ – Kronecker delta function
τ_{ij} – viscous stress tensor, [kgm^{-1}s^{-2}]
ω – specific dissipation rate, [c^{-1}]

Subscript

k – Kolmogorov scale

References

[1] Armaroli, N., Balzani, V., The Future of Energy Supply: Challenges and Opportunities, *Angewandte Chemie International Edition*, *46* (2007), 1-2, pp. 52-66
[2] Borkowicz, R., *et al.*, Dry Low NO_x Single Stage Dual Mode Combustor Construction for a Gas Turbine, Patent US5259184A, USA, 1993
[3] Waslo, J., *et al.*, Premixed Pilot Nozzle for Dry Low NO_x Combustor, Patent US4982570A, USA, 1991
[4] Fitts, D. O., Dry Low NO_x Multi-Nozzle Combustion-Liner Cap Assembly, Patent CA2091497C, Canada, 1994

[5] Joshi, N. D., Moreno, F. E., Staged Low NO_x Premix Gas Turbine Combustor, Patent US4928481A, USA, 1990
[6] Beebe, K. W., Premixing Dry Low NO_x Emissions Combustor with Lean Direct Injection of Gas Fule, Patent US6192688B1, USA, 2001
[7] Beebe, K.W. Gas Turbine Catalytic Combustor with Preburner and Low NO_x Emissions, Patent US5161366A, USA, 1992
[8] Razak, A., *Industrial Gas Turbines: Performance and Operability*, Elsevier, New York, USA, 2007
[9] Washam, R., Dry Low NO_x Combustion System for Utility Gas Turbine, *Proceedings*, 1983 Joint Power Generation Conference, GT Papers 1983, American Society of Mechanical Engineers, Indianopolis, Ind., USA, 1983
[10] Davis, L., Washam, R., *Development of a Dry Low NO_x Combustor*, ASME paper, New York, USA, 1989, p. 255
[11] Chen, H., *et al*., Engine Combustion and Emission Fuelled with Natural Gas, *Journal of the Energy Institute*, *92* (2018), 4, pp. 1123-1136
[12] Yize, L., *et al*., Review of Modern Low Emissions Combustion Technologies for Aero Gas Turbine Engines, *Progress in Aerospace Sciences*, *94* (2017), Oct., pp. 12-45
[13] Konnov, A. A., *et al*., The NO_x Formation, Control and Reduction Thechniques, Handbook of Combustion, in: *Combustion Diagnostics and Pollutants*, Wiley, New York, USA, 2010, Vol. 2, pp. 439-464
[14] Dostiyarov, A. M., *et al*., Numerical Modelling of the Influence of Different Options for Feeding Fuel on the Combustion Process for Turbine Profiles, in: IOP Conference Series: *Earth and Environmental Science*, *274* (2019), 1, pp. 38-44
[15] Reijnder, J., *et al*., Investigation of Direct-Injection Via Micro-porous Injector Nozzle, *Proceeding*s, 4th Euro Combustion Meeting, Vienna, Austria, 2009
[16] Tanner, F. X., Srinivasan, S., Gradient-Based Optimization of a Multi-Orifice Asynchronous Injection System in a Diesel Engine Using an Adaptive Cost Function, SAE Technical Paper, 2006-01-1551, 2006
[17] Park, S. W., Reitz, R. D., Modelling the Effect of Injector Nozzle-Hole Lay-out on Diesel Engine Fuel Consumption and Emissions, *Journal of Engineering for Gas Turbines and Power*, *130* (2008), 3, pp. 1-10
[18] Keiczek, H., Multi-Hole Injection Nozzle, Patent US4202500A, USA, 1980
[19] Park, S. W., Reitz, R. D., Optimization of Fuel/Air Mixture Formation for Stoichiometric Diesel Combustion Using a 2-Spray-Angle Group-Hole Nozzle, *Fuel*, *88* (2009), 5, pp. 843-852
[20] Zhang, Y., *et al*., Spray Characteristics of a Group-Hole Nozzle for Direct-Injection Diesel Engines, *Atomization and Sprays*, *16* (2006), 1, pp. 35-50
[21] Zhang, W., *et al*., An Experimental Study on Fiat-Wall-Impinging Spray of Microhole Nozzles under Ultra-High Injection Pressures, Proceedings of the Institution of Mechanical Engineers – Part D: *Journal of Automobile Engineering*, *222* (2008), 9, pp. 1731-1741
[22] Gupta, A. K., *et al*., *Swirl Flows*: Abacus Press, London, UK, 1984
[23] Syred, N., Beer, J., Combustion in Swirling Flows: A Review, *Combustion and Flame*, *23* (1974), 2, pp. 143-201
[24] Dostyarov, A. M., *et al*., Micromodular Air Injectors for the Annular Combustion Chamber of a Gas Turbine Engine (in Russian), *Herald of KazNRTU*, *115* (2019), 6, pp. 451-456
[25] Meier, W., *et al*., Investigations of Swirl Flames in a Gas Turbine Model Combustor, *Combustion and Flame*, *144* (2006), 1, pp. 225-236
[26] Tennekes, H., Lumley, J. L., *A First Course in Turbulence*, MIT Press, Cambridge, Mass., USA, 1972
[27] Bradshaw, P., *An Introduction Turbulence and Its Measurement*, Elsevier Science & Technology, New York, USA, 1971, p. 218
[28] Menter, F. R., Two-Equation Eddy-Viscosity Turbulence Models for Engineering Applications, *AIAA Journal*, *32* (1994), 8, pp. 1598-1605
[29] ***, FLUENT 6.2 Users Guides: Lebanon, USA, 2005

Paper submitted: August 31, 2020
Paper revised: January 18, 2021
Paper accepted: January 18, 2021